Gyrokinetic water-bag modeling of a plasma column: Magnetic moment distribution and finite Larmor radius effects

R. Klein, E. Gravier, P. Morel, N. Besse, and P. Bertrand
IJL, UMR 7198, CNRS–Nancy Université, F-54506 Vandoeuvre-lès-Nancy Cedex, France

(Received 2 April 2009; accepted 15 June 2009; published online 25 August 2009)

Describing turbulent transport in fusion plasmas is a major concern in magnetic confinement fusion. It is now widely known that kinetic and fluid descriptions can lead to significantly different properties. Although more accurate, the kinetic calculation of turbulent transport is much more demanding of computer resources than fluid simulations. An alternative approach is based on a water-bag representation of the distribution function that is not an approximation but rather a special class of initial conditions, allowing one to reduce the full kinetic Vlasov equation into a set of hydrodynamics equations while keeping its kinetic character [P. Morel, E. Gravier, N. Besse *et al.*, Phys. Plasmas **14**, 112109 (2007)]. In this paper, the water-bag concept is used in a gyrokinetic context to study finite Larmor radius effects with the possibility of using the full Larmor radius distribution instead of an averaged Larmor radius. The resulting model is used to study the ion temperature gradient (ITG) instability. © *2009 American Institute of Physics*.
[DOI: 10.1063/1.3174926]

I. INTRODUCTION

It is now well established that transport coefficients in magnetic fusion confinement are strongly influenced by microinstabilities[1,2] such as low-frequency ion temperature gradient (ITG) turbulence[2,3] or collisionless trapped electron modes,[4–6] which are the origin of anomalous transport. These instabilities are driven by equilibrium density gradient and by ion and electron equilibrium temperature gradient as well. Several works, using both fluid[7–9] and gyrokinetic[10–15] description to study ion turbulence in tokamaks, have recently been performed.

It is now widely known that kinetic and fluid descriptions can lead to significantly different properties, such as the instability threshold and the linear growth rate.

On one hand, fluid codes are reported to overestimate turbulent transport level.[16–18] As a matter of fact, comparison between the fluid and gyrokinetic approach, studying a three dimensional kinetic interchange instability shows that the distribution function can be far from a Maxwellian one.[19] This is in contradiction from the usual assumption of a fluid closure.[19] Moreover, wave-particle resonant processes can certainly play an important role because phase velocity and ion thermal velocity can be sufficiently close to each other.

On the other hand, although more accurate, the kinetic calculation of turbulent transport is much more demanding of computer resources than fluid simulations. Furthermore, solving kinetic equations is still a nontrivial task.[5,6,14,20–22] This motivated us to revisit an alternative approach based on the water-bag (WB) representation.

Introduced initially by DePackh,[23] Feix and co-workers,[24–26] this model was extended into a double WB by Berk and Roberts,[27] and Finzi,[28] and generalized to the multiple WB (MWB).[26,29–31] The MWB model was shown to bring the link between fluid and kinetic descriptions of a collisionless plasma, allowing one to keep the kinetic aspect of the problem with the same complexity as a multifluid model.

In recent works,[32,33] we used the WB description in the framework of gyrokinetic modeling (gyro-WB, i.e., GWB model). First, a linear study of ITG instability has been performed in the case of the drift-kinetic approximation in cylindrical geometry without taking into account FLR effects, leading to results[32] very close to that obtained in Ref. 14. Nonlinear numerical simulation has also been carried out.[33] Furthermore, a linear study of both collisional drift waves and ITG has been discussed in the case of a linear magnetic plasma device.[34] Indeed, in order to point out kinetic effects on drift waves, interesting results obtained with our GWB model have been compared with a fluid model.[35,36]

The next step, which is the aim of the present paper, is to go beyond the drift-kinetic approximation by taking into account finite Larmor radius (FLR) effects in the GWB model.

Our model has been successfully compared to the classical treatment of FLR effects[37] in the case of a Maxwellian distribution. Since the WB allows to deal with any distribution, the ITG instability has been studied in the case of a non-Maxwellian distribution function. The precise shape of the perpendicular distribution is shown to have an important effect on the instability threshold and linear growth rate.

II. GYROKINETIC EQUATIONS AND WATER-BAG MODELING

A. The gyrokinetic model

In magnetized plasma fusion devices, electromagnetic fluctuations occur on time scales much longer than charged particle gyromotion ($\omega/\Omega_c \ll 1$, where ω is the fluctuation frequency and Ω_c the cyclotron frequency). Moreover, the wavelength of these fluctuations is much smaller than the characteristic scale length of magnetic field $B/|\nabla B|$, density $n/|\nabla n|$, and temperature $T/|\nabla T|$ gradients. This gyrokinetic ordering[38] allows separation between fast gyromotion and slow dynamics in the perpendicular direction to the magnetic field, resulting in a reduction in the six-dimensional phase space into a three dimensional (in space) and two dimensional (in velocity). The particles are then described by a statistical distribution function $f_{GC}(\mathbf{r},v_\parallel,\mu,t)$ of their guiding-center (GC) position. The variable $v_\parallel$ is the velocity in the parallel direction to the magnetic field and $\mu = mv_\perp^2/2B$ is the magnetic moment (the first adiabatic invariant), which is linked to the perpendicular dynamics.

In this paper, the following hypotheses are assumed:

- A cylindrical geometry is considered, with an axial, homogeneous, and stationary magnetic field ($\mathbf{B}=B_o\mathbf{u}_z$).
- Inertia and FLR effects on electrons are neglected: their response to low-frequency fluctuations is adiabatic: $n_e = n_{eo}e^{e\phi/k_BT_e}$.
- Collisions are neglected.

The nonlinear gyrokinetic equations that describe the time evolution of the ion gyrocenter distribution function f_{GC} then writes[38–41]

$$\frac{\partial f_{GC}}{\partial t} + \mathbf{v_D}\cdot\nabla f_{GC} + \frac{dv_\parallel}{dt}\frac{\partial f_{GC}}{\partial v_\parallel} = 0, \tag{1}$$

$$\mathbf{v_D} = v_\parallel \mathbf{u}_z - \frac{\nabla \mathcal{J}_\mu \phi \times \mathbf{u}_z}{B_o}, \tag{2}$$

$$\frac{dv_\parallel}{dt} = -\frac{q_i}{m_i}\nabla \mathcal{J}_\mu \phi \cdot \mathbf{u}_z, \tag{3}$$

$$\frac{d\mu}{dt} = 0, \tag{4}$$

where $q_i = Z_i e$ and m_i are the ion charge and mass. The symbol $\mathcal{J}_\mu$ represents the gyroaverage operator. This operator takes into consideration the fact that particles do not lie on their GC; due to their gyromotion, they explore points in space in which the electric field acting on them is not the same as that of their GC. The gyroaverage operator depends on the Larmor radius $r_L(\mu)$ and writes[37]

$$\mathcal{J}_\mu F(\mathbf{r}) = \frac{1}{2\pi r_L(\mu)}\int F(\mathbf{R})\,\delta[|\mathbf{R}-\mathbf{r}| - r_L(\mu)]d\mathbf{R}, \tag{5}$$

where $F(\mathbf{r})$ is the function to be averaged, and with the expression of the Larmor radius, $r_L^2 = 2\mu/q_i\Omega_{ci}$.

The quasineutrality equation writes as follows:

$$n_{eo}\exp\left(\frac{e\phi}{k_BT_e}\right) = Z_i\left[\int_0^\infty d\mu \mathcal{J}_\mu n_{i\mu} + \nabla_\perp\cdot\left(\frac{n_{io}}{\Omega_{ci}B_o}\nabla_\perp\phi\right)\right], \tag{6}$$

where

$$n_{i\mu} = \int_{-\infty}^{\infty} dv_\parallel f_{GC} \tag{7}$$

and where $\nabla_\perp\cdot[(n_{io}/\Omega_{ci}B_o)\nabla_\perp\phi]$ is the polarization drift correction to the ion density,[14] and n_{io} is the equilibrium ion density. This correction to the ion density is valid in the long wavelength approximation.

The drift-kinetic equation, which is equivalent to the $\mu=0$ case, coupled with quasineutrality equation $n_e = Z_i n_i$ (where $n_i = \int_0^\infty d\mu \int_{-\infty}^{\infty} dv_\parallel f_{GC}$), describes a plasma dynamics with no FLR effects.

In the gyrokinetic description, $v_\parallel$ is a kinetic variable, whereas the ion magnetic moment $\mu = m_i v_\perp^2/2B_o$, because of its invariance, is just a label defining different particle classes, each of them having a different Larmor radius. Therefore, we can consider an initial preparation of the ion distribution by forming different particle groups, each one having a discrete μ value.[42] Because of the μ-invariance, the distribution function can be written,

$$f_{GC}(\mathbf{r},v_\parallel,\mu,t) = \sum_{k=1}^{N} f_{GC}^{\mu_k}(\mathbf{r},v_\parallel,t)\,\delta(\mu-\mu_k)\Delta\mu. \tag{8}$$

In this description, a discrete magnetic moment set $\{\mu_k\}_{k=1,\ldots,N}$ is considered, together with a discrete Larmor radius set $\{r_{Lk}\}_{k=1,\ldots,N}$ linked by the relation $\mu = q_i r_L^2 \Omega_{ci}/2$. The $\Delta\mu$ value depends on the density of the μ-sampling. A regular grid, $\mu_k = (k-1/2)\Delta\mu$ with $\Delta\mu = \mu_N/(N-1/2)$, is considered.

The interest of this invariance is that the different particle groups do not mix with each other because actually no differential operation is acting on μ. The knowledge of the asymptotic μ-distribution function in [Eq. (8)], by considering a finite number of magnetic moment values, will allow us to save both computation time and memory space in numerical codes.

B. The water-bag model

The reader can refer to Refs. 32–34 for a detailed presentation of the GWB model, in particular, the method for choosing WB parameters and the application of the model for ITG instabilities. As seen above, gyrokinetic modeling makes full use of the μ-invariance to eliminate perpendicular kinetic variables in the Vlasov equation. In the same way, the WB concept uses Liouville's invariance to reduce again the phase space dimension.

Implementation of WB concept consists in using a stepwise distribution function of the following form (refer to Fig. 1):

$$f_{\mathrm{MWB}}(\mathbf{r},v_\parallel,\mu,t) = \sum_{k=1}^{N}\sum_{j=1}^{M} A_{jk}\{H[v_\parallel - v_{jk}^-(\mathbf{r},t)] - H[v_\parallel - v_{jk}^+(\mathbf{r},t)]\}\,\delta(\mu-\mu_k)\Delta\mu, \tag{9}$$

where $j=1,\ldots,M$ and $k=1,\ldots,N$.

The most interesting property of the WB distribution is the absolute time invariance of the different bag heights A_{jk}.

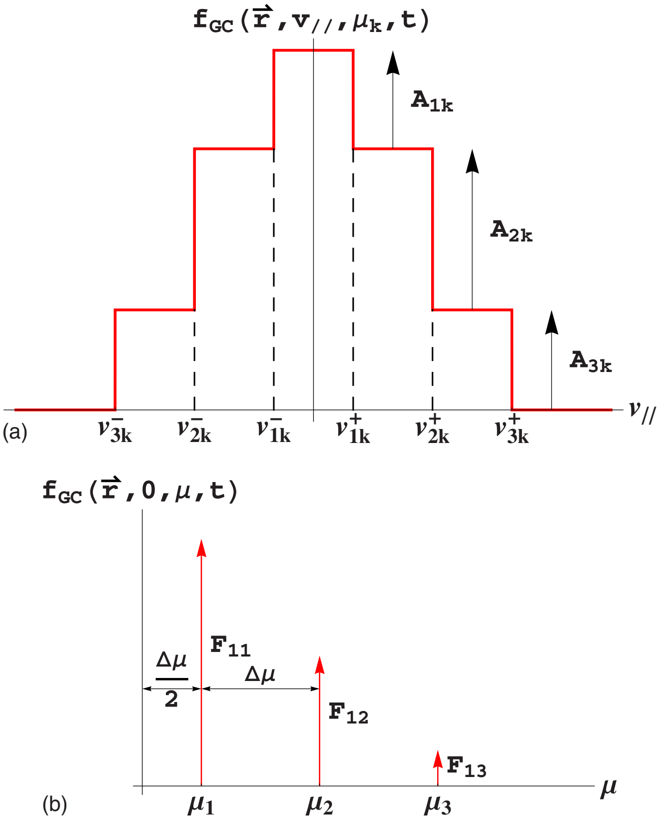

FIG. 1. (Color online) Parallel (a) and perpendicular (b) MWB distributions as a function of $v_\parallel$ and μ for $M=3$ and $N=3$.

Consequently, the evolution of the system is entirely determined by the dynamical equations of the finite set of contours $v^+_{jk}(\mathbf{r},t)$ and $v^-_{jk}(\mathbf{r},t)$.

The gyrokinetic equations [Eqs. (1) and (6)] lead to the following set of equations:

$$\frac{\partial v^\pm_{jk}}{\partial t} - \frac{\nabla_\perp \mathcal{J}_{\mu_k}\phi \times \mathbf{u}_z}{B_o} \cdot \nabla_\perp v^\pm_{jk} + v^\pm_{jk}\nabla_\parallel v^\pm_{jk} \cdot \mathbf{u}_z = -\frac{q_i \nabla_\parallel \mathcal{J}_{\mu_k}\phi}{m_i} \cdot \mathbf{u}_z, \tag{10}$$

which are coupled only by the quasineutrality equation

$$n_{eo} \exp\left(\frac{e\phi}{k_B T_e}\right) = Z_i\left[\sum_{k=1}^{N} \mathcal{J}_{\mu_k} n_{ik}\Delta\mu + \nabla_\perp \cdot \left(\frac{n_{io}}{\Omega_{ci}B_o}\nabla_\perp \phi\right)\right], \tag{11}$$

with

$$n_{ik} = \sum_{j=1}^{M} A_{jk}(v^+_{jk} - v^-_{jk}). \tag{12}$$

In these equations, j is nothing but a label (exactly in the same way than k) since no differential operation is carried on $v_\parallel$. What we actually do is to bunch together particles within the same bag j, the same magnetic moment μ_k, and let each bag evolve using contours equations [Eq. (10)]. Of course the different bags are coupled through the quasineutrality equation [Eq. (11)].

To sum up, introducing both magnetic moment and Liouville invariance appears as an exact reduction in the phase space dimension (elimination of $v_\parallel$ and $v_\perp$). Of course these eliminated velocities reappear in the various magnetic moments $\{\mu_k\}_{k=1,\ldots,N}$ and bags $j=1,\ldots,M$, needing a special initial preparation of the plasma (Dirac masses for μ and Lebesgue subdivision for $v_\parallel$).

Since there is no mathematical lower bound on N and M, from a physical point of view, many interesting results can be obtained even with reasonably small numbers for N and M. Although this fact is commonly used in gyrokinetics, the further WB reduction should afford more analytical approaches, which are not restricted to Maxwellian distribution functions. Furthermore, the double sampling (j,k) allows to consider any *arbitrary* distribution. This is particularly important in the perspective to revisit FLR effects with less analytic and numerical effort, which is the goal of this paper.

III. ITG INSTABILITY WITH FINITE LARMOR RADIUS EFFECTS

In this section, a linear analysis is performed on GWB equations and generalizes the work performed in the drift-kinetic case.[32] The goal is to study FLR effects on ITG instabilities. The important point is that no hypothesis is carried on the particular shape of the μ-distribution.

In this paper a cylindrical symmetric plasma is considered in which equilibrium parameters depend only on the radial variable r. In [Eq. (10)], which describes contours dynamics, we now use a Fourier-mode development of the form:

- $v^\pm_{jk}(r,\theta,z,t) = \pm a_{jk}(r) + \delta v^\pm_{jk}(r)\exp^{-i(\omega t - m\theta - k_\parallel z)}$,
- $\phi(r,\theta,z,t) = 0 + \delta\phi(r)\exp^{-i(\omega t - m\theta - k_\parallel z)}$,

where m is the orthoradial mode, with $k_\theta = m/r$.

In the radial direction, the Fourier modes are not proper modes of the system; we need to approximate the radial profile of perturbations in order to obtain the dispersion relation. According to numerical computation and experiment,[35,36,43] we chose the profile defined as an exponential function, such that

$$\delta\phi(r) = e^{g(r)}\delta\phi_o, \tag{13}$$

$$\delta v_{jk}(r) = e^{g(r)}\delta v_{jko}, \tag{14}$$

with

$$g(r) = -(r - r_o)^2/\Delta r^2. \tag{15}$$

The value of r_o and Δr are assumed to represent the shape of the radial perturbations.

Substituting these expressions in Eqs. (10) and (6) and using the equilibrium quasineutrality equation, $n_{eo} = Z_i n_{io}$ allow to obtain the linearized GWB equations, which leads to the following dispersion relation of the system:

$$\varepsilon(\omega,k_\theta,k_\parallel) = 1 + Z_i\rho_s^2[\kappa(r) + k_\theta^2] - \Delta\mu\sum_{j,k}\frac{J_{ok}^2\alpha_{jk}}{\omega^2 - k_\parallel^2 a_{jk}^2}[Z_i\omega_{cs}^2 + \omega\omega_{jk}^*], \qquad (16)$$

with $\rho_s=c_s/\Omega_{ci}$, $c_s^2=k_BT_e/m_i$, $\omega_{cs}=k_\parallel c_s$, $\alpha_{jk}=2A_{jk}a_{jk}$, $\omega_{jk}^*=-k_\theta\frac{k_BT_e}{eB_o}\kappa_{jk}$, and $\kappa(r)=-\{\partial_r^2 g+(\partial_r g)^2+[(1/r)+\kappa_N]\partial_r g\}$. We defined $J_{ok}=J_o(k_\theta\sqrt{2\mu_k/Z_ie\Omega_{ci}})$, where J_o is the zero order Bessel function of the first kind and represents the gyroaverage operator in Fourier space.

Let us now recall the method allowing to determine the physically relevant MWB parameters.[32] The ion equilibrium distribution function is chosen to be an even function of $v_\parallel$ and can be written as

$$f_{GC}(r,v_\parallel,\mu) = \sum_{k=1}^{N}\frac{n_{io}}{v_{Ti}^3}P\left(\frac{v_\parallel}{v_{Ti}},\frac{\mu}{v_{Ti}^2}\right)\delta(\mu-\mu_k)\Delta\mu, \qquad (17)$$

where $P(x,y)$ is a normalized function of x and y, and n_{io} and $v_{T_i}=\sqrt{k_BT_i/m_i}$ are equilibrium quantities depending on r. We want to approach this function by the following WB distribution function. A regular grid in $v_\parallel$ is chosen $a_j=(j-1/2)\Delta a$ with $\Delta a=a_M/(M-1/2)$.

$$f_{\mathrm{MWB}}(r,v_\parallel,\mu) = \sum_{j=1}^{M}\sum_{k=1}^{N}A_{jk}[H(v_\parallel + a_j(r)) - H(v_\parallel - a_j(r))]\delta(\mu-\mu_k)\Delta\mu. \qquad (18)$$

Let us define the moments of the distribution function

$$\mathfrak{M}_l(f) = \int_0^\infty d\mu\int_{-\infty}^{\infty}dv_\parallel v_\parallel^l f(r,v_\parallel,\mu). \qquad (19)$$

For the continuous distribution function, one gets

$$m_l = \mathfrak{M}_l(f_{GC}) = \int_0^\infty d\mu\int_{-\infty}^{\infty}dv_\parallel v_\parallel^l f_{GC}(r,v_\parallel,\mu), \qquad (20)$$

while for the MWB function

$$m_l^{\mathrm{MWB}} = \mathfrak{M}_l(f_{\mathrm{MWB}}) = \frac{\Delta\mu}{l+1}\sum_{j,k}2A_{jk}a_j^{l+1} = \frac{n_{io}\Delta\mu}{l+1}\sum_{j,k}\alpha_{jk}a_j^l. \qquad (21)$$

By taking the radial derivative of Eq. (20) and using Eq. (17), it can be shown that

$$\partial_r m_l = \left[\kappa_N + \frac{l}{2}\kappa_T\right]m_l, \qquad (22)$$

where $\kappa_N=(1/n_{io})\partial_r n_{io}$ and $\kappa_T=(1/T_i)\partial_r T_i$.

Performing the radial derivative of m_l^{MWB} yields

$$\partial_r m_l^{\mathrm{MWB}} = \Delta\mu\sum_{j,k}2A_{jk}a_j^l\partial_r a_j = n_{io}\Delta\mu\sum_{j,k}\alpha_{jk}\kappa_{jk}a_j^l, \qquad (23)$$

where $\kappa_{jk}=(1/a_j)\partial_r a_j$ is linked to density and temperature equilibrium gradients and can be written as a linear combination,

$$\alpha_{jk}\kappa_{jk} = \frac{\beta_{jk}}{2}\kappa_T + \gamma_{jk}\kappa_N. \qquad (24)$$

The unknown coefficients α_{jk}, β_{jk}, and γ_{jk} obey the following system:

$$\sum_{j,k}\alpha_{jk}a_j^l = \frac{(l+1)}{n_{io}\Delta\mu}m_l, \qquad (25)$$

$$\sum_{j,k}\beta_{jk}a_j^l = \frac{l}{n_{io}\Delta\mu}m_l, \qquad (26)$$

$$\sum_{j,k}\gamma_{jk}a_j^l = \frac{1}{n_{io}\Delta\mu}m_l. \qquad (27)$$

A Taylor expansion of f_{GC} in m_l allows one to write these parameters as a function of f_{GC} values.

If we define: $F_{jk}=(n_{io}/v_{Ti}^3)P(a_j-\Delta a/2,\mu_k)$, we can show that

$$\alpha_{jk} = \frac{2(F_{jk}-F_{j+1k})a_j}{n_{io}}, \qquad (28)$$

$$\beta_{jk} = \alpha_{jk} - \gamma_{jk}, \qquad (29)$$

$$\gamma_{jk} = \Delta a\frac{F_{jk}+F_{j+1k}}{n_{io}}, \qquad (30)$$

$$\alpha_{jk}\kappa_{jk} = \frac{\beta_{jk}}{2}\kappa_T + \gamma_{jk}\kappa_N, \qquad (31)$$

where

$$A_{jk} = F_{jk} - F_{j+1k}. \qquad (32)$$

To simplify algebra, it is interesting to consider the following form where $v_\parallel$ and μ dependence are separated.

$$f_{GC}(r,v_\parallel,\mu) = \sum_{k=1}^{N}\frac{n_{io}}{v_{Ti}^3}S\left(\frac{v_\parallel}{v_{Ti}}\right)T\left(\frac{\mu}{v_{Ti}^2}\right)\delta(\mu-\mu_k)\Delta\mu, \qquad (33)$$

allowing to obtain a simplified form of these MWB parameters in which j and k are separated.

Using the same method as previously, we define

$$F_{jk} = \lambda_k\frac{n_{io}}{v_{Ti}}S\left(\frac{a_j-\Delta a/2}{v_{Ti}}\right) \qquad (34)$$

with

$$\lambda_k = \frac{T(\mu_k/v_{Ti}^2)}{v_{Ti}^2}. \qquad (35)$$

Then we get

$$\alpha_{jk} = \lambda_k\alpha_j, \qquad (36)$$

$$\beta_{jk} = \lambda_k\beta_j, \qquad (37)$$

$$\gamma_{jk} = \lambda_k\gamma_j, \qquad (38)$$

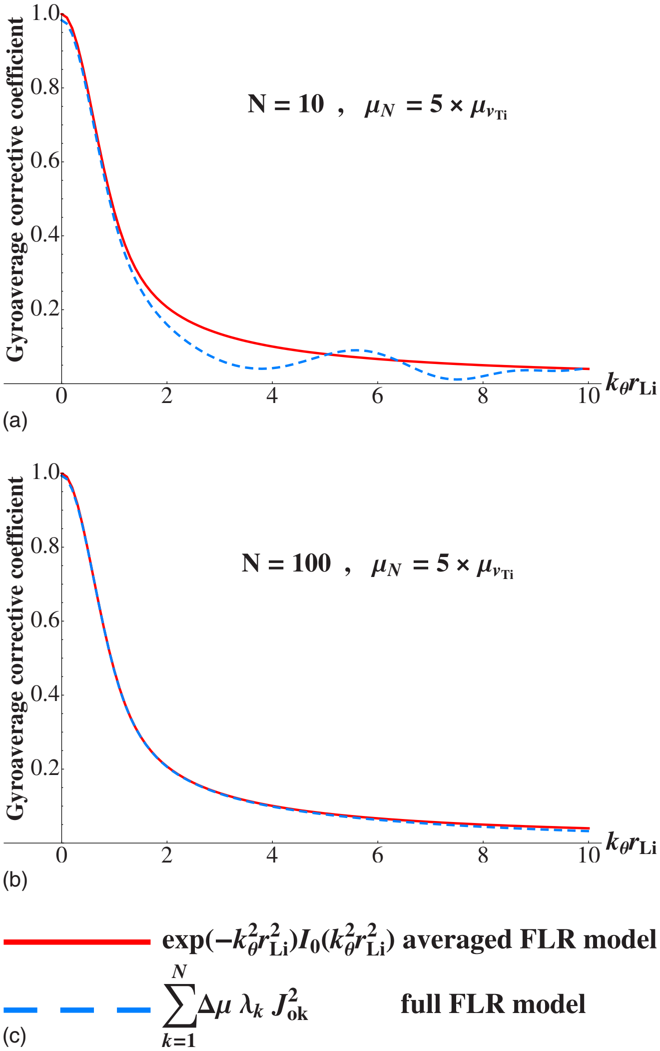

FIG. 2. (Color online) Gyroaverage corrective coefficient plotted against $k_\theta r_{Li}$. The parameter $\mu_{v_{Ti}} = m_i v_{Ti}^2 / 2B_o$ is the thermal magnetic moment.

$$\kappa_{jk} = \kappa_j, \tag{39}$$

where

$$\alpha_j = \frac{2(F_j - F_{j+1})a_j}{n_{io}} = \frac{2A_j a_j}{n_{io}}, \tag{40}$$

$$\beta_j = \alpha_j - \gamma_j, \tag{41}$$

$$\gamma_j = \Delta a \frac{F_j + F_{j+1}}{n_o}, \tag{42}$$

$$\kappa_j = \left(\frac{\beta_j}{2} \kappa_T + \gamma_j \kappa_N \right) / \alpha_j, \tag{43}$$

$$A_{jk} = \lambda_k A_j = F_{jk} - F_{j+1k}. \tag{44}$$

These expressions provide a general method for any arbitrary equilibrium MWB parameters.

IV. MAXWELLIAN CASE

In order to validate the classical treatment of gyroaverage effects, we compare our results in the case of a Maxwellian perpendicular distribution function with a classical averaged treatment of the perpendicular distribution. This treatment consists in using a modified gyroaverage operator by averaging it over a Maxwellian,[37]

$$\mathcal{I}_o = \int J_o^2\left(k_\theta \sqrt{\frac{2\mu(v_\perp)}{Z_i e \Omega_{ci}}} \right) \exp^{-m_i v_\perp \hat{A}1/2k_B T_i} v_\perp dv_\perp$$
$$= \exp^{-k_\theta^2 r_{Li}^2} I_o(k_\theta^2 r_{Li}^2), \tag{45}$$

where $r_{Li} = v_{Ti}/\Omega_{ci}$ is the thermal Larmor radius and I_o is the modified Bessel function of the first kind.[37]

It must be noticed that the averaged function is not J_o but J_o^2 because the gyroaverage operator appears in this form in the dispersion relation. When using this treatment, the dispersion function can be easily obtained:

$$\varepsilon(\omega, k_\theta, k_\parallel) = 1 + Z_i \rho_s^2 [\kappa(r) + k_\theta^2]$$
$$- \mathcal{I}_o \sum_j \frac{\alpha_j}{\omega^2 - k_\parallel^2 a_j^2} [Z_i \omega_{cs}^2 + \omega \omega_j^*]. \tag{46}$$

In Eq. (46), the magnetic moment distribution is averaged. Now we want to compare it with the full FLR effects treatment obtained by using a Maxwellian perpendicular distribution function f_{GC} in the separated form [Eq. (33)] and introduce it in our GWB model. In this case the dispersion function writes

$$\varepsilon(\omega, k_\theta, k_\parallel) = 1 + Z_i \rho_s^2 [\kappa(r) + k_\theta^2]$$
$$- \sum_{k=1}^{N} \Delta\mu \lambda_k J_{ok}^2 \sum_{j=1}^{M} \frac{\alpha_j}{\omega^2 - k_\parallel^2 a_j^2} [Z_i \omega_{cs}^2 + \omega \omega_j^*], \tag{47}$$

with $\omega_j^* = -k_\theta (k_B T_e / eB_o) \kappa_j$.

The only difference between the two dispersion relations Eqs. (46) and (47)) is the corrective coefficient linked to the gyroaverage effect. Consequently, the comparison between the $\Sigma_k \Delta\mu \lambda_k J_{ok}^2$ term in Eq. (47) with its corresponding term $\mathcal{I}_o$ in Eq. (46) allows us to measure the difference between the two corresponding models.

On Fig. 2, both coefficients values for different N values are plotted as a function of $k_\theta r_{Li}$. The agreement is excellent when $k_\theta r_{Li} < 1$, even for N as small as 10. Furthermore, the precision quickly increases with N. When $k_\theta r_{Li} > 1$, it is necessary to take a more dense set of magnetic moment values: the reason is that for large k in the sum $\Sigma_k \Delta\mu \lambda_k J_{ok}^2$, the argument of J_{ok} is greater than 1, and then is located in the region where Bessel's function is oscillating: obtaining a better precision needs to take a much more dense sampling. This study shows that the usual "averaged" description of gyroaverage effects gives a good description if the velocity distribution function in the perpendicular direction is a Maxwellian one.

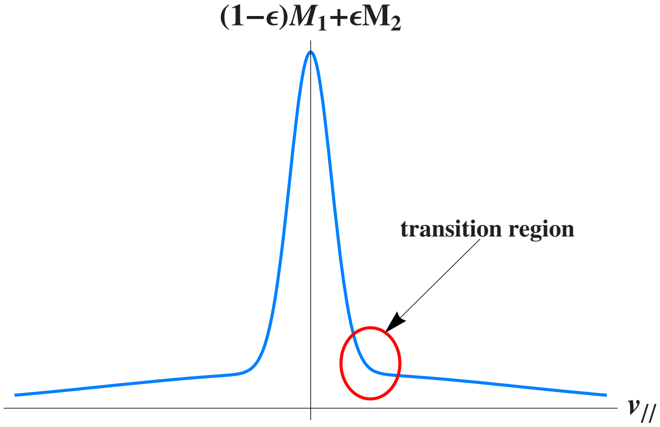

FIG. 3. (Color online) Instability threshold plotted against κ_N and κ_T with bag number $M=25$, $a_{\max}=5*v_{T_{\parallel 2}}$, magnetic moments number $N=150$, and $\mu_N=25\times\mu_{v_{T_{\parallel 2}}}$. Curve 1 (continuous line) is the instability threshold with averaged FLR effects [Eq. (47)] with $T_\perp=\langle T\rangle$. Curve 2 (dotted line) is the instability threshold with full FLR effects [Eq. (16)] and with $T_{\perp 1}=T_{\parallel 1}$ and $T_{\perp 2}=T_{\parallel 2}$.

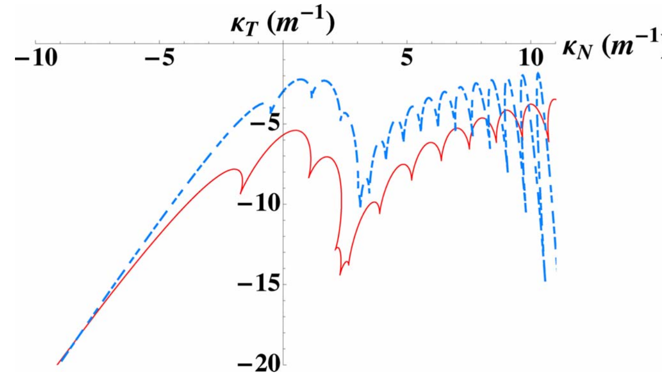

FIG. 4. (Color online) Bi-Maxwellian distribution function. The transition region where particles at temperature T_2 become majority is noted.

V. NON-MAXWELLIAN EQUILIBRIUM AND ITG INSTABILITY

The interesting point is that studying any distribution with the GWB model allows us to perform an accurate description with no more analytic and numerical complexity. In this paragraph, we study the case of a non-Maxwellian distribution function and shows that considering the full μ-distribution leads to significant improvement as compared to the classical treatment where an averaged form is used.

As an example of non-Maxwellian distribution function, a bi-Maxwellian one can be considered:

$$f_{GC}(r,v_\parallel,\mu)=\sum_{k=1}^{N}[(1-\epsilon)M_1(r,v_\parallel,\mu)+\epsilon M_2(r,v_\parallel,\mu)]\delta(\mu-\mu_k)\Delta\mu,$$

where $0\le\epsilon\le 1$,

$$M_1(r,v_\parallel,\mu)=\frac{n_{io}B_o}{m_i v_{T_{\perp 1}}^2 v_{T_{\parallel 1}}\sqrt{2\pi}}\exp\left[-\frac{\mu B_o}{k_B T_{\perp 1}}\right]\times\exp\left[-\frac{m_i v_\parallel^2}{2k_B T_{\parallel 1}}\right],$$

and

$$M_2(r,v_\parallel,\mu)=\frac{n_{io}B_o}{m_i v_{T_{\perp 2}}^2 v_{T_{\parallel 2}}\sqrt{2\pi}}\exp\left[-\frac{\mu B_o}{k_B T_{\perp 2}}\right]\times\exp\left[-\frac{m_i v_\parallel^2}{2k_B T_{\parallel 2}}\right].$$

The ion density is defined by

$$n_{io}=\int f_{GC}(r,v_\parallel,\mu)dv_\parallel d\mu.$$

This case corresponds to an energetic population in the parallel direction immersed in a core plasma. The shape of this distribution function is represented on Fig. 3.

The different temperatures being *a priori* different, the distribution function is not separable and we have to use Eq. (16) to get a dispersion relation. To simplify the analysis, it is interesting to consider the case $T_{\perp 1}=T_{\perp 2}=T_\perp$ allowing to use the dispersion relation Eq. (47).

It has been shown that computing the instability threshold in the plane (κ_N,κ_T) is equivalent to solve the following system (as explained in Ref. 32):

$$\varepsilon(\omega,k_\theta,k_\parallel)=0, \tag{48}$$

$$\partial_\omega\varepsilon(\omega,k_\theta,k_\parallel)=0. \tag{49}$$

The instability threshold is plotted in Fig. 4 for $\epsilon=0.5$, using physical parameters which will be typical of an ITER tokamak plasma: $T_e=T_{\parallel 1}=10$ keV, $T_{\parallel 2}=10\times T_{\parallel 1}$, $n_{io}=10^{20}$ m^{-3}, $B_o=5$ T, $Z_i=1$, $m_i=3.4\times10^{-27}$ kg (deuterium plasma), $k_\parallel=10^{-1}$ m^{-1}, $k_\theta=4\times10^{2}$ m^{-1}, $m=100$, $r_o=r=2.5\times10^{-1}$ m, and $\Delta r=10^{-1}$ m.

Curve 1 is obtained using the averaged FLR operator; the magnetic moment distribution is supposed to be a Maxwellian one, with an averaged temperature $\langle T\rangle=(1-\epsilon)T_{\parallel 1}+\epsilon T_{\parallel 2}$. Curve 2 corresponds to the full FLR case [Eq. (16)], when a full description of the magnetic moment distribution is performed: it is the most accurate description of FLR effects.

Furthermore, the growth rate for the dispersion relation with averaged FLR ("+" symbol) and with full FLR ("*" symbol) is plotted in Fig. 5 as a function of κ_T for $\kappa_N=-1$ m^{-1}. The impact of the full FLR consideration is enlightened. For example, with $\kappa_T=-10$ m^{-1}, the growth rate for full Larmor radius distribution is $\gamma_{\text{fullFLR}}=2.22\gamma_{\text{avgFLR}}$, where γ_{avgFLR} is the growth rate in the averaged Larmor radius case. The increase due to total FLR consideration corresponds to 122%. If the hypothesis of a Maxwellian magnetic moment distribution was fully satisfied, both growth rates would have been very close to each other; no important improvement would be carried on by considering precise shape of the μ-distribution. Now the difference between these two growth rate shows how it is important to take into account this precise shape in this case. It must be noticed that for the same set of parameters, but with $\epsilon=0.1$, the distribution function is near a Maxwellian one. In this case the difference between average and full FLR model is

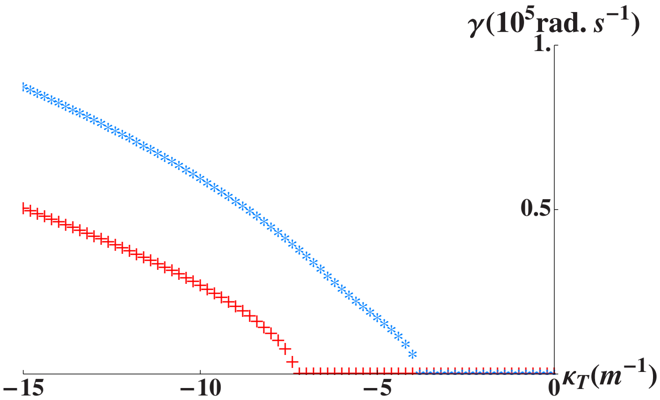

FIG. 5. (Color online) Maximum linear growth rate plotted against κ_T for $\kappa_N=-1$ m^{-1} and $\epsilon=0.5$ with $M=25$, $a_{\max}=5*v_{T_{\|2}}$, $N=150$, and $\mu_N=25*\mu_{\langle v_T\rangle}$, where $\mu_{\langle v_T\rangle}$ is the magnetic moment for the average thermal velocity at temperature $\langle T\rangle$. The (+) curve corresponds to the averaged FLR case and the (*) curve to the full FLR case.

only 11%. This result confirms that using the full FLR model is important only when the distribution function is far from a Maxwellian one.

When the distribution function is close to a Maxwellian one, the averaged FLR model is physically sufficient and numerically more effective.

VI. CONCLUSION

Our previous works[32–34] have shown how the multi-WB model, using Liouville invariance, offers an accurate description of plasma dynamics, even for a number of bags as small as 5 or 10. On the ITG example, one clearly saw that a $M=10$ description allows a good description of linear modes,[32] as well as nonlinear dynamics.[33] As a result, the WB model appears to be an interesting alternative to usual fluid and gyrokinetic descriptions of magnetized plasmas. The present paper strengthens these statements by introducing FLR in the GWB model.

The moment equivalence method between continuous distribution function and MWB,[32] which allows one to obtain physically relevant WB parameters, has been improved and adapted to a ion population with a magnetic moment distribution. The main result of this paper is that the accurate magnetic moment distribution is needed to correctly describe plasma instabilities when the distribution function is not a Maxwellian one.

Let us now remember that transport coefficient can be estimated using the mixing length approach.[2] This approach conduces to transport coefficients proportional to the maximum linear growth rate. Even if it conduces to a rough indication and nonlinear simulations would be required to confirm the linear trend, taking into account the precise shape of the μ-distribution then appears to be an important step in the determination of precise turbulent transport coefficients, depending on physical parameters.

The GWB approach allows an analytical treatment of gyrokinetic equations which results in a better comprehension of underlying physics. This linear study is a preliminary step to a complete nonlinear modeling of GWB equations; different works are in progress to explore this way. Adaptation to toroidal geometry, which does not involve any further conceptual difficulties, is also worked on.

[1] A. M. Dimits, G. Bateman, M. A. Beer, B. I. Cohen, W. Dorland, G. W. Hammett, C. Kim, J. E. Kinsey, M. Kotschenreuther, A. H. Kritz, L. L. Lao, J. Mandrekas, W. M. Nevins, S. E. Parker, A. J. Redd, D. E. Shumaker, R. Sydora, and J. Weiland, Phys. Plasmas **7**, 969 (2000).
[2] X. Garbet, Plasma Phys. Controlled Fusion **43**, A251 (2001).
[3] R. E. Waltz, Phys. Fluids **31**, 1962 (1988).
[4] H. Nordman, J. Weiland, and A. Jarmén, Nucl. Fusion **30**, 983 (1990).
[5] L. Villard, S. J. Allfrey, A. Bottino, M. Brunetti, G. L. Falchetto, V. Grandgirard, R. Hatzky, J. Nähurenberg, A. G. Peeters, O. Sauter, S. Sorge, and J. Vaclavik, Nucl. Fusion **44**, 172 (2004).
[6] T. Dannert and F. Jenko, Phys. Plasmas **12**, 072309 (2005).
[7] W. Dorland and G. W. Hammet, Phys. Fluids B **5**, 812 (1993).
[8] X. Garbet and R. E. Waltz, Phys. Plasmas **3**, 1898 (1996).
[9] G. Manfredi and M. Ottaviani, Phys. Rev. Lett. **79**, 4190 (1997).
[10] S. E. Parker, W. W. Lee, and R. A. Santoro, Phys. Rev. Lett. **71**, 2042 (1993).
[11] R. D. Sydora, V. K. Decyk, and J. M. Dawson, Plasma Phys. Controlled Fusion **38**, A281 (1996).
[12] Z. Lin, T. S. Hahm, W. W. Lee, W. M. Tang, and R. B. White, Phys. Plasmas **7**, 1857 (2000).
[13] G. Depret, X. Garbet, P. Bertrand, and A. Ghizzo, Plasma Phys. Controlled Fusion **42**, 949 (2000).
[14] V. Grandgirard, M. Brunetti, P. Bertrand, N. Besse, X. Garbet, P. Gendrih, G. Manfredi, Y. Sarazin, O. Sauter, E. Sonnendrücker, J. Vaclavik, and L. Villard, J. Comput. Phys. **217**, 395 (2006).
[15] J. Candy and R. E. Waltz, J. Comput. Phys. **186**, 545 (2003).
[16] B. Coppi, M. N. Rosenbluth, and R. Z. Sagdeev, Phys. Fluids **10**, 582 (1967).
[17] W. Horton, D. Choi, and W. M. Tang, Phys. Fluids **24**, 1077 (1981).
[18] F. Romanelli and S. Briguglio, Phys. Fluids B **2**, 754 (1990).
[19] Y. Sarazin, V. Grandgirard, E. Fleurence, X. Garbet, Ph. Ghendrih, P. Bertrand, and G. Depret, Plasma Phys. Controlled Fusion **47**, 1817 (2005).
[20] W. W. Lee, Phys. Fluids **26**, 556 (1983).
[21] A. Ghizzo, P. Bertrand, E. Fijalkow, M. R. Feix, and M. Shoucri, J. Comput. Phys. **108**, 105 (1993).
[22] X. Garbet, Y. Sarazin, V. Grandgirard, G. Dif-Pradalier, G. Darmet, Ph. Gendrih, P. Angelino, P. Bertrand, N. Besse, E. Gravier, P. Morel, E. Sonnendrücker, N. Crouseilles, J. M. Dischler, G. Latu, E. Violard, M. Brunetti, S. Brunner, X. Lapillone, T. Tran, L. Villard, and M. Boulet, Nucl. Fusion **47**, 1206 (2007).
[23] D. C. DePackh, J. Electron. Control **13**, 417 (1962).
[24] M. R. Feix, F. Hohl, and L. D. Staton, in *Nonlinear Effects in Plasmas*, edited by G. Kalmann and M. R. Feix (Gordon and Breach, New York, 1969), pp. 3–21.
[25] P. Bertrand and M. R. Feix, Phys. Lett. **28A**, 68 (1968).
[26] P. Bertrand and M. R. Feix, Phys. Lett. **29A**, 489 (1969).
[27] H. L. Berk and K. V. Roberts, in *Methods in Computational Physics*, edited by B. Alder, S. Fernbach, and M. Rotenberg (Academic, New York, 1970), Vol. 9, p. 29.
[28] U. Finzi, Plasma Phys. **14**, 327 (1972).
[29] P. Bertrand, Ph.D. thesis, Université de Nancy, France, 1972.
[30] P. Bertrand, J. P. Doremus, G. Baumann, and M. R. Feix, Phys. Fluids **15**, 1275 (1972).
[31] P. Bertrand, M. Gros, and G. Baumann, Phys. Fluids **19**, 1183 (1976).
[32] P. Morel, E. Gravier, N. Besse, R. Klein, A. Ghizzo, P. Bertrand, X. Garbet, P. Ghendrih, V. Grandgirard, and Y. Sarazin, Phys. Plasmas **14**, 112109 (2007).
[33] N. Besse, P. Bertrand, P. Morel, and E. Gravier, Phys. Rev. E **77**, 056410 (2008).
[34] E. Gravier, R. Klein, P. Morel, N. Besse, and P. Bertrand, Phys. Plasmas **15**, 122103 (2008).
[35] R. F. Ellis and E. Marden-Marshall, Phys. Fluids **22**, 2137 (1979).
[36] E. Marden-Marshall, R. F. Ellis, and J. E. Walsh, Plasma Phys. Controlled Fusion **28**, 1461 (1986).

[37] F. R. Hansen, G. Knorr, J. P. Lynov, H. L. Pecseli, and J. Juul Rasmussen, Plasma Phys. Controlled Fusion **31**, 173 (1989).
[38] T. S. Hahm, Phys. Fluids **31**, 2670 (1988).
[39] T. S. Hahm, W. Lee, and A. Brizard, Phys. Fluids **31**, 1940 (1988).
[40] A. Brizard, Phys. Fluids B **1**, 1381 (1989).
[41] K. Nishikawa and M. Wakatani, *Plasma Physics*, 3rd ed. (Springer-Verlag, Berlin, Heidelberg, New York, 2000), pp. 44–47.
[42] G. Manfredi, M. Shoucri, M. R. Feix, P. Bertrand, E. Fijalkow, and A. Ghizzo, J. Comput. Phys. **121**, 298 (1995).
[43] E. Gravier, F. Brochard, G. Bonhomme, T. Pierre, and J. L. Briançon, Phys. Plasmas **11**, 529 (2004).